

# Utility of an inexpensive near-infrared camera to quantify beach surface moisture

Shannon A. Nelson, Phillip P. Schmutz \*

Department of Earth and Environmental Science, University of West Florida, Pensacola, FL, United States of America

## ARTICLE INFO

### Article history:

Received 17 September 2019

Received in revised form 5 August 2021

Accepted 8 August 2021

Available online 11 August 2021

### Keywords:

Instrument calibration

Remote sensing

Solar reflectance

Aeolian

## ABSTRACT

Surface moisture content is an essential factor that must be considered when studying aeolian sediment transport on a sandy beach. In recent years, near-infrared (NIR) remote sensing sensors have shown promise for obtaining accurate surface moisture data; however, prior studies utilized instruments with extreme costs. This study assesses the capability of an inexpensive NIR digital camera to measure surface moisture at two sandy beach environments – Tybee Island, Georgia and Pensacola Beach, Florida – that exhibit varying sediment hue characteristics. To account for temporal variations in solar atmospheric conditions, we normalized the raw sediment surface reflectance data against a white reflectance card and a sample of oven dry sand representative of each study site. This is a necessary step to account for solar atmospheric conditions. Calibration results illustrate that the NIR camera is capable of producing accurate representations of beach surface moisture; analyses from both study sites produced  $R^2$  values greater than 0.76 with error estimates at  $\pm 1$ –2% moisture. No statistical difference in calibration relationships were observed for data collected over multiple days and times of day. Calibration data for the reflectance card produced more robust relationships with smaller prediction errors than the oven dry sand analyses; however. Overall, this study illustrates that an inexpensive digital camera modified to record NIR radiation is capable of producing robust and accurate measurements of beach surface moisture.

© 2021 Elsevier B.V. All rights reserved.

## 1. Introduction

The coastal research community has long recognized that surficial moisture of the beach environment is an important control on aeolian processes, increasing transport thresholds thereby decreasing transport rates. However, accurate measurements of moisture content at the sediment bed – top few grains of the surface layer – over suitable ranges of space and time are difficult to conduct (Delgado-Fernández et al., 2009; Edwards and Namikas, 2009; Namikas et al., 2010; Nield et al., 2011; Delgado-Fernandez et al., 2012; Schmutz and Namikas, 2018; Smit et al., 2018) and thus could contribute to the high degree of variability shown between transport models and field observations of mass flux values (Davidson-Arnott et al., 2005; Davidson-Arnott et al., 2008; Udo et al., 2008; Bauer et al., 2009; Sherman and Li, 2012).

In recent years, numerous researchers have provided technical advances to our capability to quantify beach surface moisture (e.g., McKenna-Neuman and Langston, 2003; Yang and Davidson-Arnott, 2005; Nield and Wiggs, 2011; Schmutz and Namikas, 2011;

Edwards et al., 2013a, 2013b; Nolet et al., 2014; Smit et al., 2018). Yet, overall practicality of field use, expense, and/or accuracy – particularly at low moisture values – limits their usability. Accordingly, there is still a need for improvement in our ability to precisely, rapidly, and non-destructively measure beach surface moisture for aeolian applications.

This research assessed the capability of an inexpensive near-infrared (NIR) digital camera to quantify beach surface moisture. A major advantage of using the NIR wavelength spectrum, 700–3000 nanometer (nm), to measure surface moisture is that a number of wavelengths (i.e., 760, 970, 1200, 1470 and 1940 nm) have strong moisture absorption capabilities (Slaughter et al., 2001; Lobell and Asner, 2002; Weidong et al., 2002; Nolet et al., 2014). Recent studies using NIR techniques document strong correlations between beach surface moisture and infrared reflectance (Edwards et al., 2013a, 2013b; Nolet et al., 2014; Smit et al., 2018). A potential drawback, however, to the widespread adoption of this technique is the high cost (tens of thousands of dollars) of the instruments used – spectroradiometer and terrestrial laser scanner. Accordingly, more affordable methods that utilize infrared wavelengths to quantify beach surface moisture are needed. Prior studies by Röper et al. (2014) and Nield et al. (2016) used infrared digital cameras to measure surface moisture; however, neither study provided

\* Corresponding author.

E-mail address: [pschmutz@uwf.edu](mailto:pschmutz@uwf.edu) (P.P. Schmutz).

calibrations or accuracy assessments for their devices. Consequently, further research is a necessity to fully evaluate the applicability of using an inexpensive NIR camera to accurately measure beach surface moisture content.

## 2. Materials and methods

### 2.1. Camera

For this research, we used a Canon G15 Point-and-Shoot digital camera modified to detect light only within the NIR wavelength spectrum. Digital camera sensors (CMOS or CCD) are capable of detecting wavelengths between 350 nm and 1100 nm, yet most camera manufacturers install a UV (390 nm) low-pass filter and IR (700 nm) high-pass filter in front of the sensor (Vollmer et al., 2015). Our camera was modified by removing the UV and IR filters and placing an 850 nm low-pass filter in front of the sensor, consequently only wavelengths between 850 and 1100 nm are measured by the sensor. This spectral range encompasses the strong 970 nm moisture absorbing wavelength band.

### 2.2. Laboratory tests

To increase the effectiveness of accurately delineating surface moisture with infrared reflectance measured by the camera, establishing appropriate camera settings was necessary. To ascertain the criteria for the camera settings, we conducted a set of laboratory tests performed outdoors under various daylight conditions (i.e., time of day and cloud cover), sand mineralogy, and moisture conditions. Images were taken of sand samples at known moisture levels, both in direct sunlight and with the presence of clouds to imitate various field conditions. To maintain consistency, a custom white balance was set before each sample run using a white reflectance card with a rated reflectance of 95%. A variety of camera settings were tested and after numerous trials, it was determined that an ISO of 200, aperture of F8, and a shutter speed ranging between 1/60 and 1/1000 produced the greatest range in histogram values when analyzing dry to saturated sand samples. We found that changes in shutter speed had the largest influence on the exposure of the images and thus the spread of the resultant histogram. This was most impactful for lighter colored sediments due to the potential for over-exposure of the images. The purpose of conducting the laboratory tests was not to establish a concrete calibration of the NIR camera but to work out the methodological process and establish a baseline for camera settings.

### 2.3. Field methods

Data collection occurred at Tybee Island, Georgia [latitude 32.0002° N/longitude 80.8457° W] and Pensacola Beach, Florida [latitude 30.3337° N/longitude 87.1411° W]. These two beach locations were chosen due to their differences in mineralogy, specifically sediment hue. Tybee Island consists of light gray to very pale brown quartz sands that are moderately sorted with a fine to medium grain size distribution – mean 0.28 mm (phi 1.84), while the sands at Pensacola Beach are white quartz that are well sorted with a mean grain size of 0.34 mm (phi 1.55).

In total, forty-seven data sets were collected between the two beach locations, twenty-one data sets – 300 individual samples – were taken over the course of five non-consecutive days at Tybee Island and sixteen data sets – 274 individual samples – on four non-consecutive days at Pensacola Beach. Data sets were collected each day at 9:00, 11:00, 13:00, 15:00, and 17:00 at both locations, with the exception of day 1 at each site as data was only collected during midday at 13:00. Different days and times of day were chosen to test the NIR camera across a range of environmental factors, particularly changes in cloud cover and solar radiation. Each data set contains eighteen to twenty-five NIR image/moisture samples, which were taken across the beach from the dune toe to the waterline in order to encompass the full range of

beach surface moisture contents. To correlate NIR reflectance measured by the camera with true surface moisture, physical scrapings (1–3 mm depth) of the sediment surface were taken at each image location and placed in a zip-lock bag and put in a cooler until gravimetric moisture measurements could be measured.

### 2.4. Data analysis

NIR reflectance was determined for each sample by analyzing the histogram of the image taken by the NIR camera – similar methodology employed by McKenna-Neuman and Langston (2003). The histogram values for digital photographs ranges from 0 (black, pure absorption) to 255 (white, pure reflectance), thus the resultant histogram represents the intensity of reflectance of solar radiation measured by the camera sensor. By comparing the peak value of the histogram [mid-point of the bin with the largest frequency] against the measured moisture content from that sample, a calibration relationship can be obtained and used to assess the capability of the device to accurately quantify beach surface moisture content (McKenna-Neuman and Langston, 2003).

During our laboratory testing, we observed that slight changes in cloud cover had an influence on the histogram values, generally shifting the histogram curve independent of moisture content. Setting a custom white balance before each set of data collections helped minimize some of the variance associated with changes in light/solar radiation conditions. However, it did not entirely eliminate this issue nor is this process always practical in the field. To account for this variability in environmental conditions, we normalized the computed peak histogram values of the sediment surface from each image against a white reflectance card that was placed in the field of view of each data collection sample image as well as against a sample of oven-dried sand representative of each study site. The ratio of the histogram values from the sediment surface to the white reflectance card and oven-dried sand produces the relative reflectance (Edwards et al., 2013b).

Due to the exponential shape of the calibration data, we performed a natural log (ln) transformation of the response values – measured gravimetric moisture content ( $\theta_g$ ) – to meet linear regression assumptions. Linear regression analyses were conducted to assess the relative strength of the relationship and establish the coefficient of determination ( $R^2$ ). The overall accuracy of the sensor to detect surface moisture was assessed by calculating the root mean square (RMSE) error. Statistical analysis was performed and graphs were created using MATLAB 2019a. Statistical significance was defined a priori as  $p < 0.05$ .

## 3. Results

Fig. 1 illustrates the calibration relationship between the  $\ln\theta_g$  and the relative reflectance data calculated for all data samples at both beach locations. Most noticeable is that the relative reflectance values at Tybee Island are lower than those measured at Pensacola Beach for all moisture content values. For example, at a  $\ln\theta_g$  of 1.61 (equivalent to 5%  $\theta_g$ ), the relative reflectance values using the reflectance card for Tybee Island and Pensacola are 0.60 and 0.75, and at a  $\ln\theta_g$  of 2.71 (equivalent to 15%  $\theta_g$ ) reflectance values are 0.50 and 0.71, respectively. Additionally, the range in the relative reflectance values between dry and saturated sands is substantially smaller at Pensacola Beach than at Tybee Island – 0.67 to 0.90 versus 0.45 to 0.79 using the reflectance card and 0.68 to 0.98 versus 0.45 to 0.92 when using an oven dry sand sample. These findings correlate well with the concept of albedo, which stipulate that lighter colored surfaces reflect more solar radiation than darker surfaces. Consequently, the darker gray, brown sands at Tybee Island naturally reflect a lower rate of solar radiation than the white hue sands of Pensacola Beach for the same relative solar atmospheric conditions, independent of moisture content. Furthermore, the relationships for both study sites produced a negative correlation between relative reflectance and moisture content – as reflectance decreases, moisture

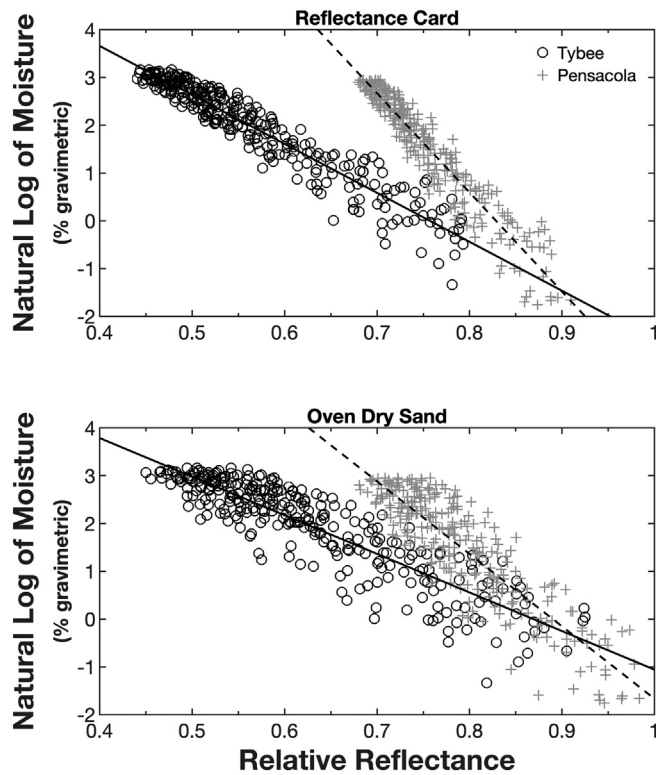


**Fig. 1.** Linear calibration relationships between the natural log of measured gravimetric moisture content and the relative reflectance for both study sites. Solid and dashed lines represent the best-fit relationship.

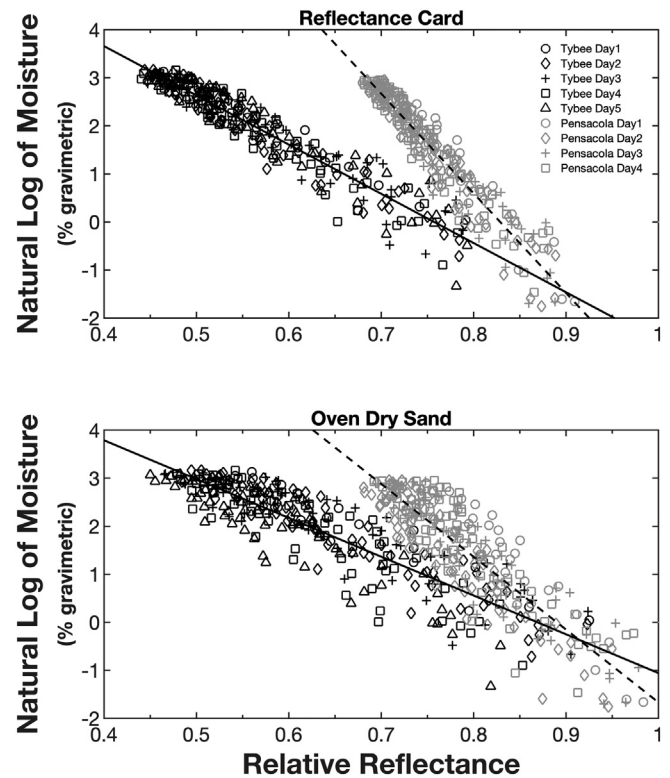


**Fig. 2.** Linear calibration relationships between the natural log of measured gravimetric moisture content and the relative reflectance for each day of data collection at both study sites. Solid and Dashed lines represent the best-fit relationship for all data samples.

content increases. This fits with well-established literature that asserts sediments with higher moisture levels absorb more incident energy, and therefore have lower reflectance values than drier sediments (Nolet et al., 2014).

We also fit relationships between  $\ln\theta_g$  and relative reflectance broken down by each individual day (Fig. 2) and the time of day (Fig. 3) of data collection. Notably, the spread of the relationships is very similar independent of the temporal structure of data collection, differences in the calibration relationships were not statistically different at  $p < 0.05$ . This signifies that the NIR camera is capable of producing repeatable measurements of beach surface moisture contents.

Tables 1 and 2 provide the coefficient of determinant ( $R^2$ ) and root mean square error (RMSE) values for all data sample runs. Regardless of the mineral hue or date/time of data collection, the calibration relationships at both study sites exhibit robust  $R^2$  values that were determined to be significant at  $p < 0.05$  and produced RMSE values of  $\pm 1$ – $2\%$   $\theta_g$ , which fall within the range of reported calibration assessments from more expensive infrared devices (Edwards et al., 2013b; Nolet et al., 2014; Smit et al., 2018). The resultant  $R^2$  values for the oven dried sand normalizing method are slightly lower compared to the reflectance card method; however, RMSE values still fall within  $\pm 1$ – $2\%$   $\theta_g$  and were not statistically different at  $p < 0.05$ . The overall low error values for both of these techniques illustrate the effectiveness of the NIR camera to accurately quantify beach surface moisture content across a range of sediment characteristics and solar conditions.

#### 4. Discussion

The functionality of digital cameras allows for quick and effective field sampling over various spatial and temporal ranges. Our data collection methodology employed point measurements of the beach surface – each sample/photo was a few 10s of  $\text{cm}^2$  in scale. However, the use of small-scale point measurements to ascertain larger spatial-temporal

trends in beach surface moisture is time-consuming thereby reducing the functionality of a digital camera, which can provide landscape scale images. The establishment of automated remote monitoring systems (e.g., Lynch et al., 2006; Darke et al., 2009; Delgado-Fernández et al., 2009; Delgado-Fernández and Davidson-Arnott, 2011; Delgado-Fernández et al., 2012) has provided assessments of the spatial and temporal changes in beach surface moisture and allowed researchers to quickly assess changes in aeolian fetch area thereby increasing our ability to quantify beach/dune sediment budgets and assess landscape dynamics over longer time periods. However, these studies have primarily utilized standard RGB cameras employing the surface brightness technique developed by McKenna-Neuman and Langston (2003). Our study shows that installing a NIR camera within these remote monitoring systems could improve the accuracy of these systems in establishing spatial-temporal surface moisture trends.

Moreover, the use of unmanned aerial vehicles (UAVs), which have the capability to carry a variety of sensors (i.e., LIDAR, IR, and visible cameras) and measure large spatial areas (upwards of a few hundred hectares) within a few hours at centimeter scale resolution, offers an opportunity to tie highly detailed spatiotemporal surface moisture information with beach topography through the use of Structure for Motion (SfM) applications. UAVs have been used in a variety of coastal beach and dune geomorphic research in recent years (e.g., Nolet et al., 2017; Guisado-Pintado et al., 2019; Laporte-Fauret et al., 2019); however, to date UAVs have yet to be employed to quantify moisture content of the beach surface. Our results indicate that the inclusion of NIR sensors on UAVs provides promising advancement in our ability to monitor larger-scale spatial-temporal beach moisture trends.

Utilizing these sensors to monitor larger-scale spatial-temporal beach moisture trends either via remote monitoring stations or UAVs requires normalizing the raw sediment surface reflectance data to account for solar atmospheric conditions. Researchers have acknowledged

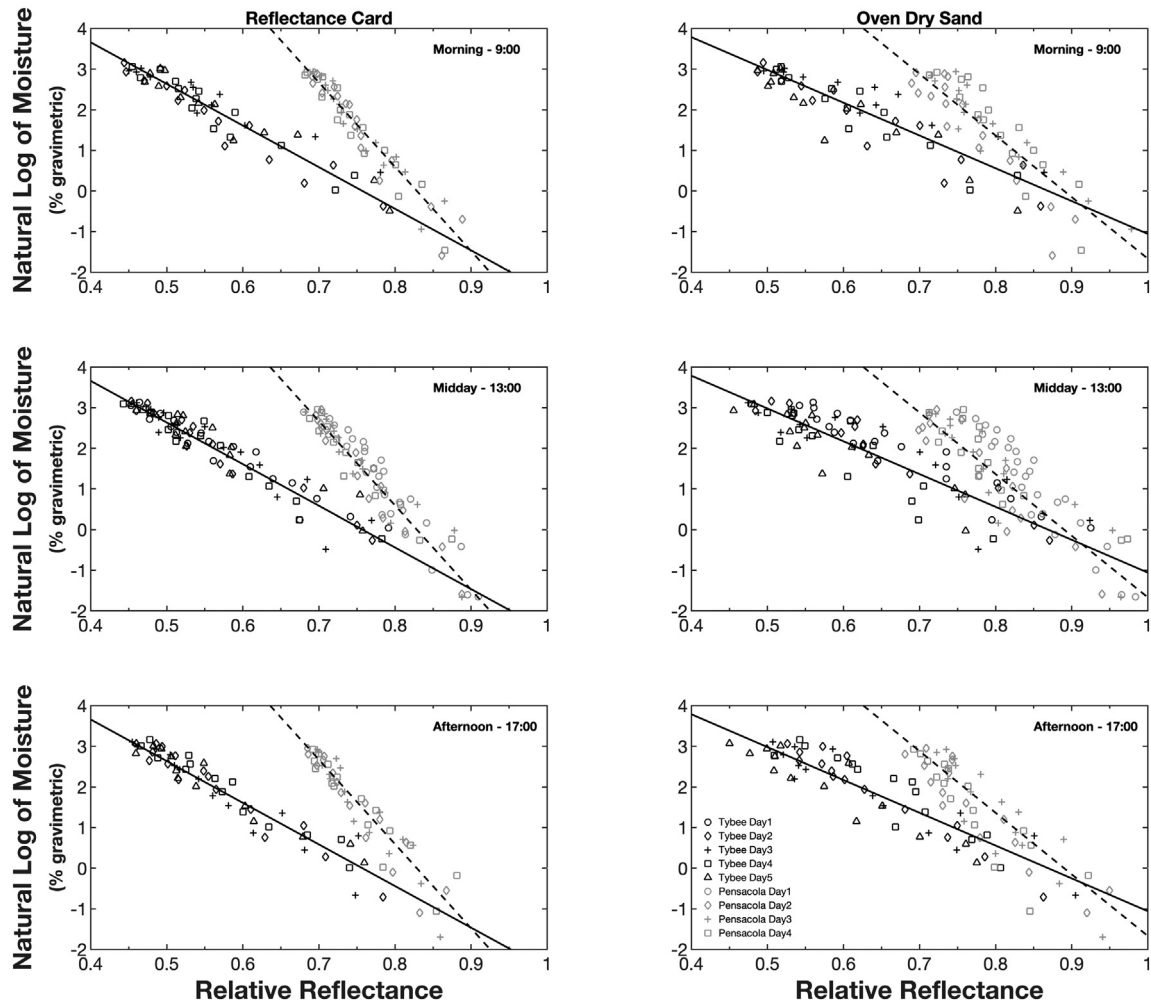


**Fig. 3.** Linear calibration relationships between the natural log of measured gravimetric moisture content and the relative reflectance for both study sites for data collected each day in the morning (9:00), midday (13:00), and afternoon (17:00) at both study sites. Solid and Dashed lines represent the best-fit relationship for all data samples.

this and developed techniques to minimize or even eliminate these impacts. Edwards et al. (2013a) sought to remove the influence of all external environmental factors by encapsulating an NIR sensor within a PVC tube. Although effective, with reported error values around 1%, this setup is not practical as it eliminates any potential use to establish meso-scale spatial-temporal trends within a remote monitoring station or for placement on a UAV. McKenna-Neuman and Langston (2003, 2006) chose to account for the influence of variable solar conditions by normalizing their data against a gray-scale reflectance card. We followed the methodology employed by McKenna-Neuman and Langston (2003, 2006) in our study, but utilized a white reflectance card with a 95% rated reflectance as well as a sample of oven-dried sand from each study site. Calibration data from the reflectance card produced more robust relationships with smaller prediction errors than the oven dry sand analyses. Although differences were not statistically different at  $p < 0.05$ , the long-term placement of an oven dry sand sample within the field of view of the camera may not be practical due to field/atmospheric constraints (i.e., changes in humidity).

A limitation of using an inexpensive NIR camera is that it is a passive sensor and therefore cannot be used at night. Commercial NIR night-vision cameras use low energy IR lights for illumination, allowing the sensor to detect IR reflectance at night. A potential solution for nighttime use at a remote monitoring site could be the installation of IR floodlights. This, however, would necessitate the construction of a new set of calibrations to establish the relationship

between the artificial illumination and measured surface moisture content.

## 5. Conclusions

The results of this study demonstrate that surface moisture on a sandy beach can be accurately quantified using an inexpensive near-infrared digital camera. Calibrations between gravimetric moisture and NIR reflectance at each of our two beach locations produced very strong ( $R^2 > 0.76$ ) statistically significant relationships with error estimates at  $\pm 1$ –2% moisture, which is a notable improvement in accuracy over visible wavelength studies and compares with research using more expensive NIR devices. Normalizing the raw sand surface reflectance data is paramount to account for variations in solar atmospheric conditions caused by changing cloud cover and temporal (i.e., seasonal, daily or hourly – morning/midday/afternoon) radiation differences. Accordingly, data showed no statistical difference in the calibration relationship at both study sites for samples collected over multiple days and times of day. This signifies that the NIR camera is capable of producing repeatable measurements of beach surface moisture contents. Based on our data and the practicality of use in the field at a remote monitoring station or with a UAV, we recommend normalizing surface reflectance data against a reflectance card placed within the field of view. Although differences were not statistically different, the calibration relationships for the reflectance card produced smaller moisture prediction errors.



**Table 1**

Coefficient of determination ( $R^2$ ) values as well as the  $\ln\theta_g$  and  $\theta_g$  root mean square error (RMSE) values for all data sample runs at Tybee Island derived from a linear fit calibration model after a natural log transformation of moisture content values. All data runs are significant at  $p < 0.05$ .

|             |             | Tybee            |                    |                 |               |                    |                 |
|-------------|-------------|------------------|--------------------|-----------------|---------------|--------------------|-----------------|
|             |             | Reflectance card |                    |                 | Oven dry sand |                    |                 |
|             |             | $R^2$            | $\ln\theta_g$ RMSE | $\theta_g$ RMSE | $R^2$         | $\ln\theta_g$ RMSE | $\theta_g$ RMSE |
| All samples |             | 0.91             | 0.30               | 1.35            | 0.80          | 0.45               | 1.57            |
| Day 1       | 13:00       | 0.94             | 0.24               | 1.27            | 0.91          | 0.29               | 1.34            |
| Day 2       | 9:00        | 0.94             | 0.28               | 1.33            | 0.88          | 0.39               | 1.48            |
|             | 11:00       | 0.95             | 0.22               | 1.25            | 0.93          | 0.26               | 1.30            |
|             | 13:00       | 0.96             | 0.23               | 1.25            | 0.90          | 0.29               | 1.34            |
|             | 15:00       | 0.94             | 0.25               | 1.28            | 0.92          | 0.29               | 1.34            |
|             | 17:00       | 0.95             | 0.26               | 1.30            | 0.91          | 0.27               | 1.31            |
|             | All samples | 0.94             | 0.26               | 1.30            | 0.90          | 0.33               | 1.39            |
| Day 3       | 9:00        | 0.93             | 0.22               | 1.24            | 0.89          | 0.25               | 1.29            |
|             | 11:00       | 0.96             | 0.22               | 1.24            | 0.87          | 0.38               | 1.46            |
|             | 13:00       | 0.88             | 0.39               | 1.47            | 0.76          | 0.54               | 1.72            |
|             | 15:00       | 0.95             | 0.24               | 1.27            | 0.82          | 0.43               | 1.54            |
|             | 17:00       | 0.89             | 0.39               | 1.47            | 0.88          | 0.41               | 1.51            |
|             | All samples | 0.90             | 0.32               | 1.38            | 0.82          | 0.43               | 1.53            |
| Day 4       | 9:00        | 0.92             | 0.28               | 1.32            | 0.89          | 0.33               | 1.39            |
|             | 11:00       | 0.90             | 0.38               | 1.46            | 0.77          | 0.58               | 1.79            |
|             | 13:00       | 0.94             | 0.27               | 1.31            | 0.84          | 0.44               | 1.55            |
|             | 15:00       | 0.94             | 0.24               | 1.27            | 0.83          | 0.39               | 1.48            |
|             | 17:00       | 0.94             | 0.24               | 1.27            | 0.85          | 0.40               | 1.48            |
|             | All samples | 0.91             | 0.29               | 1.34            | 0.79          | 0.45               | 1.57            |
| Day 5       | 9:00        | 0.93             | 0.29               | 1.34            | 0.87          | 0.40               | 1.49            |
|             | 11:00       | 0.93             | 0.36               | 1.43            | 0.89          | 0.37               | 1.45            |
|             | 13:00       | 0.88             | 0.31               | 1.37            | 0.83          | 0.39               | 1.47            |
|             | 15:00       | 0.89             | 0.34               | 1.40            | 0.75          | 0.51               | 1.67            |
|             | 17:00       | 0.94             | 0.25               | 1.29            | 0.89          | 0.35               | 1.41            |
|             | All samples | 0.89             | 0.34               | 1.40            | 0.85          | 0.41               | 1.50            |

## Declaration of competing interest

The authors declare that they have no known competing financial interests or personal relationships that could have appeared to influence the work reported in this paper.

**Table 2**

Coefficient of determination ( $R^2$ ) values as well as the  $\ln\theta_g$  and  $\theta_g$  root mean square error (RMSE) values for all data sample runs at Pensacola Beach derived from a linear fit calibration model after a natural log transformation of moisture content values. All data runs are significant at  $p < 0.05$ .

|             |             | Pensacola Beach  |                    |                 |               |                    |                 |
|-------------|-------------|------------------|--------------------|-----------------|---------------|--------------------|-----------------|
|             |             | Reflectance card |                    |                 | Oven dry sand |                    |                 |
|             |             | $R^2$            | $\ln\theta_g$ RMSE | $\theta_g$ RMSE | $R^2$         | $\ln\theta_g$ RMSE | $\theta_g$ RMSE |
| All samples |             | 0.91             | 0.36               | 1.43            | 0.79          | 0.55               | 1.73            |
| Day 1       | 13:00       | 0.90             | 0.41               | 1.50            | 0.86          | 0.48               | 1.61            |
| Day 2       | 9:00        | 0.93             | 0.37               | 1.45            | 0.89          | 0.47               | 1.60            |
|             | 11:00       | 0.94             | 0.32               | 1.37            | 0.89          | 0.39               | 1.47            |
|             | 13:00       | 0.89             | 0.58               | 1.79            | 0.81          | 0.74               | 2.10            |
|             | 15:00       | 0.90             | 0.34               | 1.40            | 0.77          | 0.52               | 1.69            |
|             | 17:00       | 0.91             | 0.40               | 1.49            | 0.86          | 0.51               | 1.67            |
|             | All samples | 0.92             | 0.34               | 1.40            | 0.85          | 0.48               | 1.61            |
| Day 3       | 9:00        | 0.87             | 0.46               | 1.58            | 0.80          | 0.41               | 1.51            |
|             | 11:00       | 0.89             | 0.40               | 1.49            | 0.84          | 0.40               | 1.49            |
|             | 13:00       | 0.90             | 0.41               | 1.50            | 0.81          | 0.57               | 1.77            |
|             | 15:00       | 0.92             | 0.37               | 1.44            | 0.88          | 0.44               | 1.55            |
|             | 17:00       | 0.90             | 0.41               | 1.51            | 0.83          | 0.55               | 1.72            |
|             | All samples | 0.90             | 0.38               | 1.45            | 0.85          | 0.46               | 1.59            |
| Day 4       | 9:00        | 0.93             | 0.33               | 1.39            | 0.79          | 0.51               | 1.66            |
|             | 11:00       | 0.95             | 0.27               | 1.30            | 0.84          | 0.39               | 1.47            |
|             | 13:00       | 0.92             | 0.30               | 1.35            | 0.78          | 0.51               | 1.66            |
|             | 15:00       | 0.91             | 0.36               | 1.43            | 0.86          | 0.35               | 1.42            |
|             | 17:00       | 0.89             | 0.41               | 1.51            | 0.78          | 0.58               | 1.78            |
|             | All samples | 0.91             | 0.34               | 1.40            | 0.78          | 0.53               | 1.71            |

## Acknowledgements

This research was funded in part by the Department of Earth and Environmental Sciences and the Office of Undergraduate Research at the University of West Florida. We wish to thank three anonymous reviewers for providing insightful comments that helped to improve the manuscript.

## References

- Bauer, B.O., Davidson-Arnott, R.G.D., Hesp, P.A., Namikas, S.L., Ollerhead, J., Walker, I.J., 2009. Aeolian sediment transport on a beach: surface moisture, wind fetch, and mean transport. *Geomorphology* 105 (1–2), 106–116. <https://doi.org/10.1016/j.geomorph.2008.02.016>.
- Darke, I., Davidson-Arnott, R., Ollerhead, J., 2009. Measurement of beach surface moisture using surface brightness. *J. Coast. Res.* 25 (1), 248–256. <https://doi.org/10.2112/07-0905.1>.
- Davidson-Arnott, R.G.D., MacQuarrie, K., Aagaard, T., 2005. The effect of wind gusts, moisture content and fetch length on sand transport on a beach. *Geomorphology* 68 (1–2), 115–129. <https://doi.org/10.1016/j.geomorph.2004.04.008>.
- Davidson-Arnott, R.G.D., Yang, Y., Ollerhead, J., Hesp, P.A., Walker, I.J., 2008. The effects of surface moisture on aeolian sediment transport threshold and mass flux on a beach. *Earth Surf. Process. Landf.* 33 (1), 55–74. <https://doi.org/10.1002/esp.1527>.
- Delgado-Fernández, I., Davidson-Arnott, R.G.D., 2011. Meso-scale aeolian sediment input to coastal dunes: the nature of aeolian transport events. *Geomorphology* 126 (1–2), 217–232. <https://doi.org/10.1016/j.geomorph.2010.11.005>.
- Delgado-Fernández, I., Davidson-Arnott, R.G.D., Ollerhead, J., 2009. Application of a remote sensing technique to the study of coastal dunes. *J. Coast. Res.* 25 (5), 1160–1167. <https://doi.org/10.2112/09-1182.1>.
- Delgado-Fernández, I., Davidson-Arnott, R.G.D., Bauer, B., Walker, I.J., Ollerhead, J., Rew, H., 2012. Assessing aeolian beach-surface dynamics using a remote sensing approach. *Earth Surf. Process. Landf.* <https://doi.org/10.1002/esp.3301>.
- Edwards, B.L., Namikas, S.L., 2009. Small-scale variability in surface moisture on a fine-grained beach: implications for modeling aeolian transport. *Earth Surf. Process. Landf.* 34 (10), 1333–1338. <https://doi.org/10.1002/esp.1817>.
- Edwards, B.L., Namikas, S.L., D'Sa, E.J., 2013a. Simple infrared techniques for measuring beach surface moisture. *Earth Surf. Process. Landf.* 38, 192–197. <https://doi.org/10.1002/esp.3319>.
- Edwards, B.L., Schmutz, P.P., Namikas, S.L., 2013b. Comparison of surface moisture measurements with depth-integrated moisture measurements on a fine-grained beach. *J. Coast. Res.* 29 (6), 1284–1291. <https://doi.org/10.2112/JCOASTRES-D-12-00008.1>.
- Guisado-Pintado, E., Jackson, D.W.T., Rogers, D., 2019. 3D mapping efficacy of a drone and terrestrial laser scanner over a temperate beach-dune zone. *Geomorphology* 328, 157–172. <https://doi.org/10.1016/j.geomorph.2018.12.013>.
- Laporte-Faure, Q., Marieu, V., Castelle, B., Michalet, R., Bujan, S., Rosebery, D., 2019. Low-cost UAV for high-resolution and large-scale coastal dune change monitoring using photogrammetry. *J. Mar. Sci. Eng.* 7 (3), 63. <https://doi.org/10.3390/jmse703063>.
- Lobell, D.B., Asner, G.P., 2002. Moisture effects on soil reflectance. *Soil Sci. Soc. Am. J.* 66, 722–727. <https://doi.org/10.2136/sssaj2002.0722>.
- Lynch, K., Jackson, D.W.T., Cooper, J.A.G., 2006. A remote-sensing technique for the identification of aeolian fetch distance. *Sedimentology* 53, 1381–1390. <https://doi.org/10.1111/j.1365-3091.2006.00808.x>.
- McKenna-Neuman, C., Langston, G., 2003. Spatial analysis of surface moisture content on beaches subject to aeolian transport. *Proceedings of the Canadian Coastal Conference, Kingston, Ontario*, pp. 1–10.
- McKenna-Neuman, C., Langston, G., 2006. Measurement of water content as a control of particle entrainment by wind. *Earth Surf. Process. Landf.* 31, 303–317.
- Namikas, S.L., Edwards, B.L., Bitton, M.C.A., Booth, J.L., Zhu, Y., 2010. Temporal and spatial variabilities in the surface moisture content of a fine-grained beach. *Geomorphology* 114, 303–310.
- Nield, J.M., Wiggs, G.F., 2011. The application of terrestrial laser scanning to aeolian saltation cloud measurement and its response to changing surface moisture. *Earth Surf. Process. Landf.* 36, 273–278. <https://doi.org/10.1002/esp.2102>.
- Nield, J.M., Wiggs, G.F., Squirrell, R.S., 2011. Aeolian sand strip mobility and protodune development on a drying beach: examining surface moisture and surface roughness patterns measured by terrestrial laser scanning. *Earth Surf. Process. Landf.* 36, 513–522. <https://doi.org/10.1002/esp.2071>.
- Nield, J.M., Wiggs, G.F., King, J., Bryant, R.G., Eckardt, F.D., Thomas, D.S.G., Washington, R., 2016. Climate-surface-pore-water interactions on a salt crusted playa: implications for crust pattern and surface roughness development measured using terrestrial laser scanning. *Earth Surf. Process. Landf.* 41, 738–753. <https://doi.org/10.1002/esp.3860>.
- Nolet, C., Poortinga, A., Roosjen, P., Bartholomeus, H., Ruessink, G., 2014. Measuring and modeling the effect of surface moisture on the spectral reflectance of coastal beach sand. *PLoS One* 9 (11), e112151. <https://doi.org/10.1371/journal.pone.0112151>.
- Nolet, C., van Puijenbroek, M., Suomalainen, J., Limpens, J., Riksen, M., 2017. UAV-imaging to model growth response of marram grass to sand burial: implications for coastal dune development. *Aeolian Res.* 31 (A), 50–61. <https://doi.org/10.1016/j.aeolia.2017.08.006>.
- Röper, T., Greskowiak, J., Massmann, G., 2014. Detecting small groundwater discharge springs using handheld thermal infrared imagery. *Ground Water* 52 (6), 936–942. <https://doi.org/10.1111/gwat.12145>.

- Schmutz, P.P., Namikas, S.L., 2011. Utility of the delta-t probe for obtaining surface moisture measurements from beaches. *J. Coast. Res.* 27 (3), 478–484. <https://doi.org/10.2112/08-1130.1>.
- Schmutz, P.P., Namikas, S.L., 2018. Measurement and modeling of the spatiotemporal dynamics of beach surface moisture content. *Aeolian Res.* 34, 35–48. <https://doi.org/10.1016/j.aeolia.2018.08.001>.
- Sherman, D.J., Li, B., 2012. Predicting aeolian sand transport rates: a reevaluation of models. *Aeolian Res.* 3 (4), 371–378. <https://doi.org/10.1016/j.aeolia.2011.06.002>.
- Slaughter, D.C., Pelletier, M.G., Upadhyaya, S.K., 2001. Sensing soil moisture using NIR spectroscopy. *Appl. Eng. Agric.* 17, 241–247. <https://doi.org/10.13031/2013.5449>.
- Smit, Y., Ruessink, G., Brakenhoff, L.B., Donker, J.J.A., 2018. Measuring spatial and temporal variation in surface moisture on a coastal beach with a near-infrared terrestrial laser scanner. *Aeolian Res.* 31, 19–27. <https://doi.org/10.1016/j.aeolia.2017.07.004>.
- Udo, K., Kuriyama, Y., Jackson, D.W.T., 2008. Observation of wind-blown sand under various meteorological conditions at a beach. *J. Geophys. Res.* 113, F04008. <https://doi.org/10.1029/2007JF000936>.
- Vollmer, M., Möllmann, K.-P., Shaw, J.A., 2015. The optics and physics of near infrared imaging. *Proceedings of Education and Training in Optics and Photonics*. Volume 97930Z <https://doi.org/10.1117/12.2223094>.
- Weidong, L., Baret, F., Xingfa, G., Qingxi, T., Lanfen, Z., Bing, Z., 2002. Relating soil surface moisture to reflectance. *Remote Sens. Environ.* 81, 238–246. [https://doi.org/10.1016/S0034-4257\(01\)00347-9](https://doi.org/10.1016/S0034-4257(01)00347-9).
- Yang, Y., Davidson-Arnott, R.G.D., 2005. Rapid measurement of surface moisture content on a beach. *J. Coast. Res.* 21 (3), 447–452. <https://doi.org/10.2112/03-0111.1>.